Chapter 3

PPy/Cholic acid composite for sensing ethanol vapour

3.1 Introduction

Bile acids are molecules with steroid structure acidic in nature, bio synthesized from cholesterol in liver and stored in gallbladder [1], which has been under intensive research in the field of pathology and pharmacology for long years. Of late, it has attracted attention of material scientists also due to their potential application as building block in designing chiral templates [2], supramolecular structure in soft material [3-5], cation and anion receptors [6-7], artificial ion channel [8] and as surfactant in nanotechnology [9]. Bile acids include a group of molecules with similar but non-identical chemical structure, with surprisingly different bio-physical properties. These have conventionally 24 carbon atoms (abbreviated $C_{24)}$ with the presence of 'non-equivalent hydroxyl group (in 3, 7 and/or 12 C) and the side chain structure supporting a carboxylic acid group; which attribute to its peculiar physical and chemical properties [10]. These hydroxyl groups form the hydrophilic face with the carboxylic group of the side chain. This forms an "inner cavity" while the outer face is hydrophobic because of the three methyl groups present there. The carboxyl and hydroxyl group can be easily modified to attach other functional groups and hence various kinds of polymers can be prepared with bile acid in the main chain, as pendent groups and also as star shaped polymers with the bile acid in the core. However, synthesis of high molecular wt. polymer with bile acid in the main chain is still a challenge [11]. Ahlheim and Hal lensleben used p-tolunesulfonic acid catalyst and high reaction temperature to obtain polymer with bile acid in the main chain [12]. The principal bile acids are Cholic Acid, Chenodeoxycholic

Acid, Glychocholic Acid, Taurocholic Acid, Deoxycholic Acid and Lithocholic Acid. In the present study, we use DBSA as an additional dopant with Iron (III) chloride to incorporate Cholic Acid in aqueous media in the polymerization of Py which eventually formed Polypyrrole / Cholic Acid blend, as observed from determination of its Mol. Weight as well as FTIR spectroscopy. The composite is characterized by FTIR spectroscopy to find out molecular bonding pattern of the monomer and dopant along with the bio-molecule. Surface morphology and the structural information are collected by microscopic study, while its sensing behavior with respect to ethanol vapour is studied by impedance measurement and also by estimation of the change in resistance on ethanol exposure.

The molecular structure of Cholic Acid is given in Fig.3.1 below.

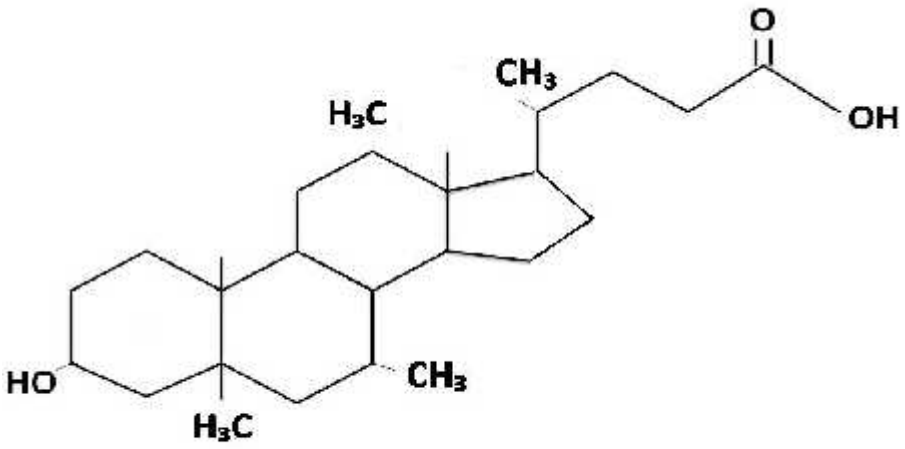

Fig 3.1 Molecular structure of Cholic acid

Mol. Weight 408.57. Chemical Formula: $C_{24}H_{40}O_5$

3.2 Experimental

3.2.1 Preparation of the PPy-Cholic Acid composite

Cholic acid is incorporated on PPy by *in-situ* co-polymerization of pyrrole. In particular, Py is taken in an aqueous medium and is subjected to sonication for 30 minutes. Cholic Acid is taken in equal weight proportion with de-ionized water and added to the Py solution. Three different samples are made in three different molar proportions of Py and Cholic Acid in 1:1, 10:1 and 100:1 molar ratio. Aqueous solution of $FeCl_3$ is added drop-wise in the Py Cholic acid mixture and the resultant solution is then subjected to magnetic stirring for two different temperatures - one at room temperature and the other at 0°C. Each sample is subjected to magnetic stirring for 90 minutes. The solution has turned greenish black immediately after addition of $FeCl_3$. The composite obtained as greenish black precipitate which is filtered and washed by de-ionized water and methanol several times to remove any oligomer, dried and then stored under vacuum. A solution of the composite is used for making thin film by spin casting. Thin films of thickness of the order of 1µ are used for characterizations of the synthesized composite.

3.2.2 Ethanol sensing

Sensitivity measurements are done by monitoring impedance response (Z) and current-voltage (I-V) characteristics of the polymer in presence of ethanol vapor, under dc and ac bias. A detector is made by pressing the polymer between two steel plates of cross section 1 cm^2 with holes in the middle. End of the stainless steel plates are connected to the source meter or the impedance analyzer according to the biasing condition. The whole system is placed in a 100 cc glass vessel kept in a desiccator.

Characterization of the composite sample is done by SEM, TEM, FT-IR and AFM. Molecular weight is determined by GPC columns. Electrical properties are studied by measuring current-voltage (I-V) characteristics in the voltage range of 0 to 1.0 V. Configuration of electrode attachment is that of a two probe method. Impedance measurement is undertaken at room temperature in the frequency range 50 Hz-500 Hz.

3.3 Results and discussion

3.3.1 FTIR spectra

The FTIR spectra are shown in Fig. 3.2 for the DBSA doped PPy and Cholic Acid incorporated composite. In PPy, the peak at 2919 cm^{-1} corresponds to S=O and at 2376 cm^{-1} corresponds to C-H stretching vibration which indicates the presence of benzenoid ring of DBSA.

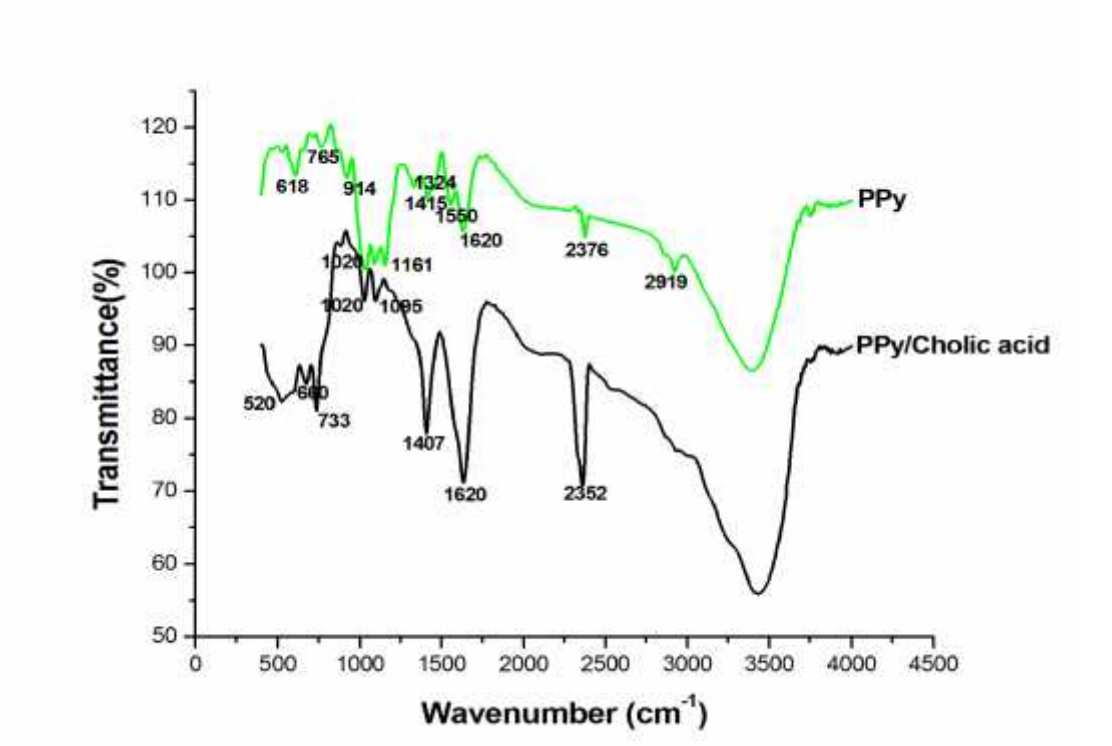

Fig. 3.2 FTIR spectra of PPy and PPy-cholic acid composite

The peaks at 1620 cm^{-1}, 1555 cm^{-1} and 1415 cm^{-1} can be associated with C-N and C-C asymmetric and symmetric ring stretching vibration. The peak at 1085 cm^{-1} and 1038 cm^{-1} are attributed to C-H deformation and N-H stretching vibration. The peak at 1150 cm^{-1} represents the S=O stretching vibration of sulfonate anions $(–SO_3)^{2-}$ which compensate the positive charge in the PPy chain [14]. The broad peaks around 1300 cm^{-1} represents the C-H and C-N in plane deformation. The characteristic PPy peaks are found in the lower wavelength region in which the peak at around 600 cm^{-1} represents C-S stretching due to sulfonate doping [15].

In the CA doped composite the sharp peak appearing at 2352 cm^{-1} is due to carboxylic group in CA. CA incorporation results in shifting and merging of PPy peaks in the range 1020-1100 cm^{-1} where the previous peaks merge giving rise to two less intense but sharp peaks at 1020 cm^{-1} and 1095 cm^{-1}, which are attributed to C=O and C-H stretching [16]. The characteristic PPy peaks at lower wavelength also merges to give a lesser no of vibrational stretching mode, which indicates the change of chemical bonding in the synthesized composite. The incorporation of CA probably results in certain complimentary bonds stronger then the covalent bond discussed later.

3.3.2 Surface morphology (SEM)

The effect of DBSA is observed in SEM image of PPy with aggregation of the particles shown in Fig.3.3 (A) while (B) represents the polymer composite with Cholic acid.

Considerable change in surface morphology of PPy is observed with the doping of Cholic acid.

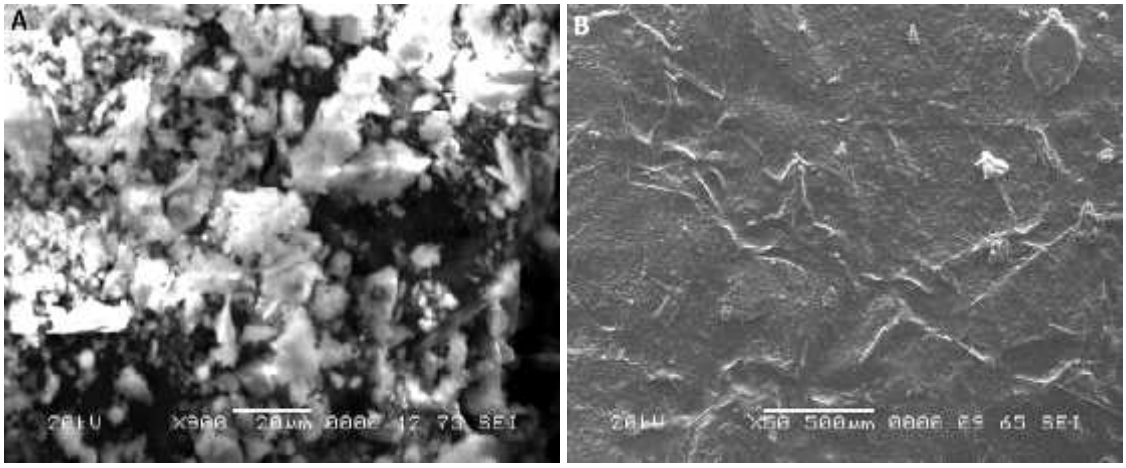

Fig. 3.3 SEM images of PPy (A) and PPy/cholic acid composite (B)

The composite morphology is converted into a layered formation with certain cavities, creating multiple layers. It may be due to surfactant effect of CA which results in multilayer formation because of interacting molecular and electrostatic forces.

3.3.3 TEM

TEM image also reveals interesting structural changes when CA is introduced in the polymer. This is shown in Fig.3.4 where (A) is the image of DBSA doped PPy without CA and (B) is that of the CA incorporated one. The PPy particles are dispersed in different forms and sometimes nucleated to make it a multi phase pattern. On introduction of CA, the image takes a completely different turn with the formation of multiple nanosheets giving it a layered

morphology. These layers are probably formed by a group of particles with similar interfacial interaction energy (E_{int}).

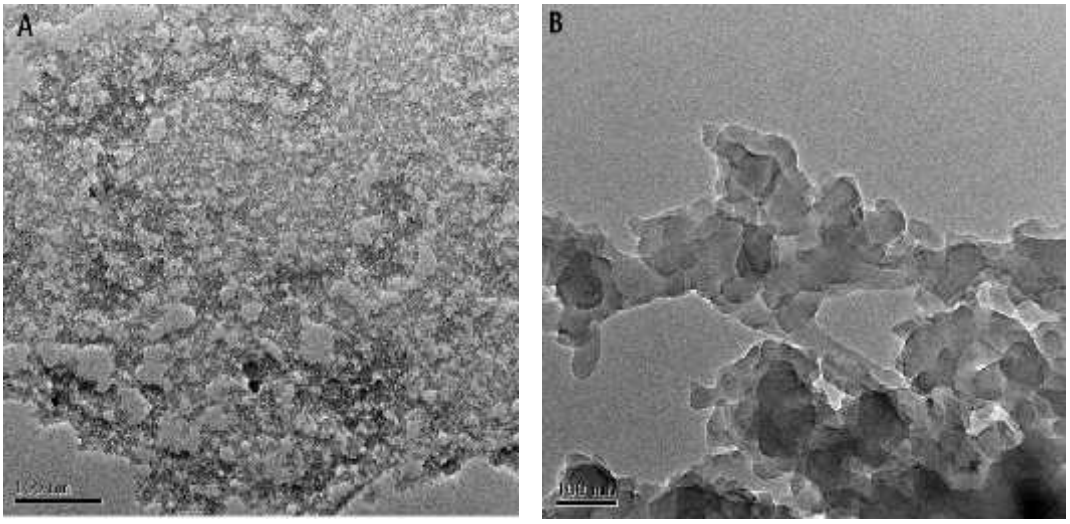

Fig.3.4 TEM images of PPy (A) and PPy/Cholic Acid composite (B)

3.3.4 AFM

The AFM images shown in Fig.3.5 ascertain the multi-layer formation in the CA incorporated composite inferred from SEM and TEM observations. The layers are extended from double layer to multiple layers giving rise to difference in conductivity of the composite which is prominent in Fig.3.8. The AFM image shows “pull-off” adhesion on PPy doped with Cholic Acid. Similar configuration has been reported earlier in PPy doped with glycoaminoglycanes (GAG) [17, 18].

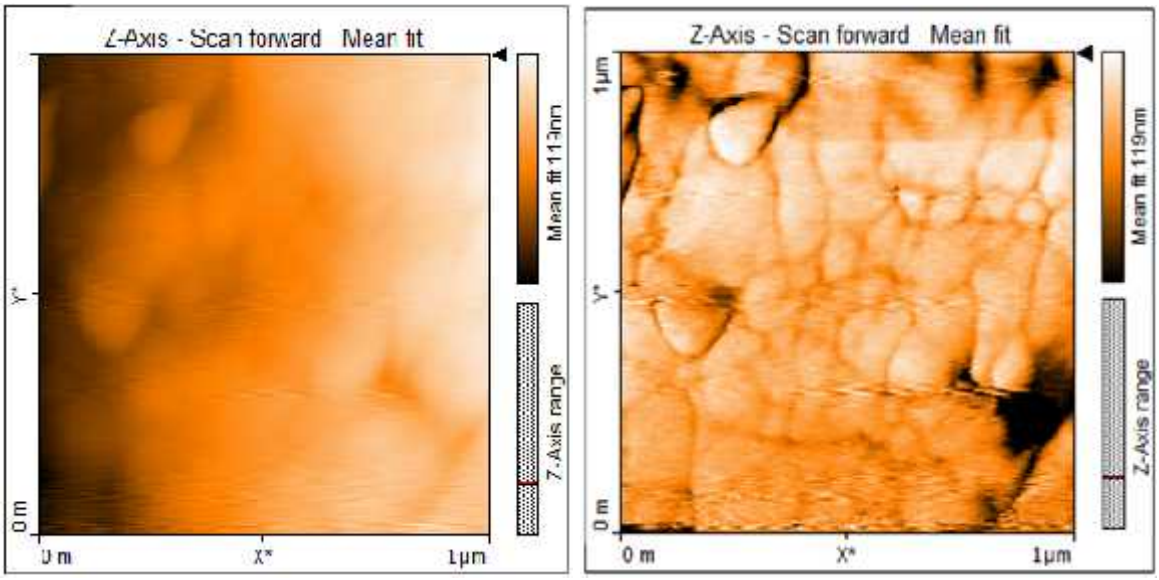

(A) **(B)**

Fig.3.5 AFM images of DBSA doped PPy (A) and PPy/Cholic Acid composite (B)

3.3.5 Molecular weight

Molecular weight of PPy and the PPy composite is estimated as:

M_n = 25,000 $gmol^{-1}$, M_w = 28,000 $gmol^{-1}$ and PDI = 0.98 for PPy.

M_n = 48,000 $gmol^{-1}$, M_w = 54,000 $gmol^{-1}$ and PDI = 1.1 for CA incorporated PPy.

Introduction of CA results in increased molecular weight. So, one can say that CA incorporation results in formation of a polymer blend with PPy. Both PPy and its composite are of uniform chain length as the PDI is around unity i.e. both the samples are mono-dispersed.

3.3.6 I-V characteristics

The d-c I-V characteristics for PPy and PPy composite in the voltage range from 0 to 1.0 V is shown in Fig. 3.6 , which shows increased slope i.e. the resistance of PPy and the PPy-CA composite is found to be decreased after ethanol intake.

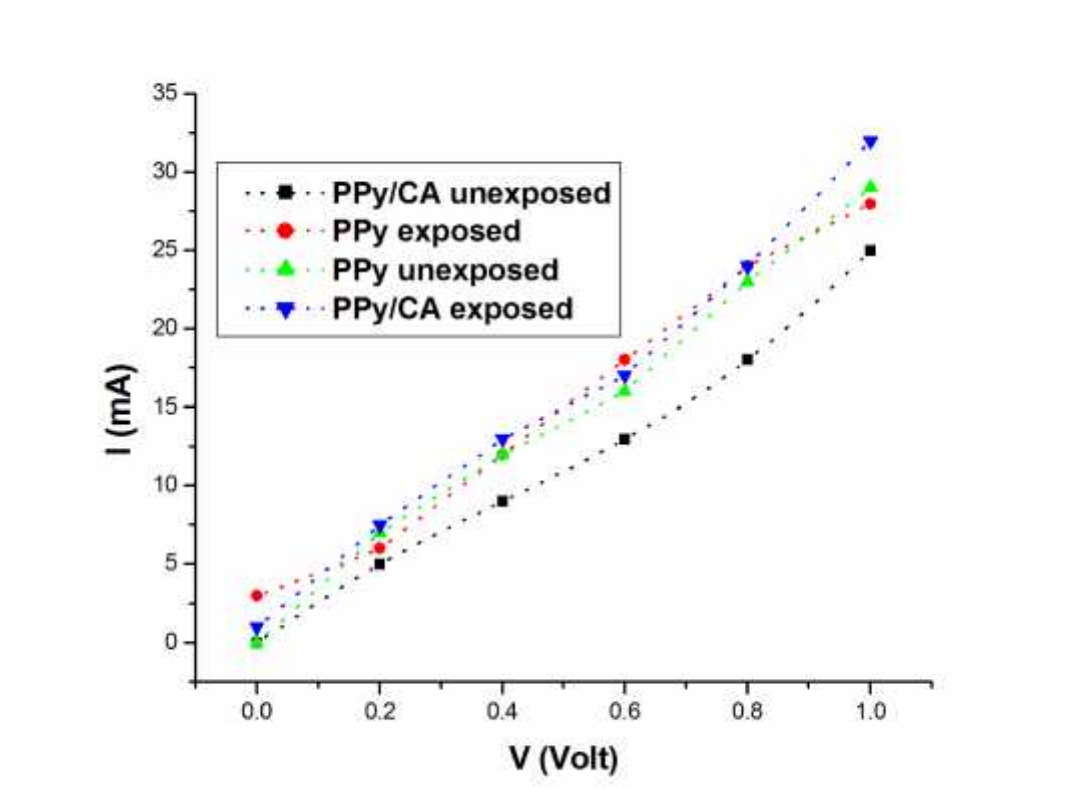

Fig. 3.6 I-V characteristics for DBSA doped PPy and PPy/ Cholic Acid composite

Resistance of PPy in unexposed state is 3.03 KOhm which changes to 0.71 KOhm, while the resistance of the polymer composite changes from 2.3 KOhm to 0.39 KOhm after exposure to ethanol vapours. Though the same order change in resistance is observed in both PPy and its composite, the resistance of the composite is lesser than PPy which facilitates electronic mobility in its both unexposed and exposed states.

3.3.7 Impedance measurement and low frequency I-V characteristics

The Nyquist plots for pure PPy and the PPy /CA composite for an applied bias of 2 V is plotted in Fig. 3.7. In the spectrum of the composite an almost vertical line appears in the lower frequencies indicating that the composite behaves like a simple capacitor which can be modeled with a finite transmission line circuit [19, 20].

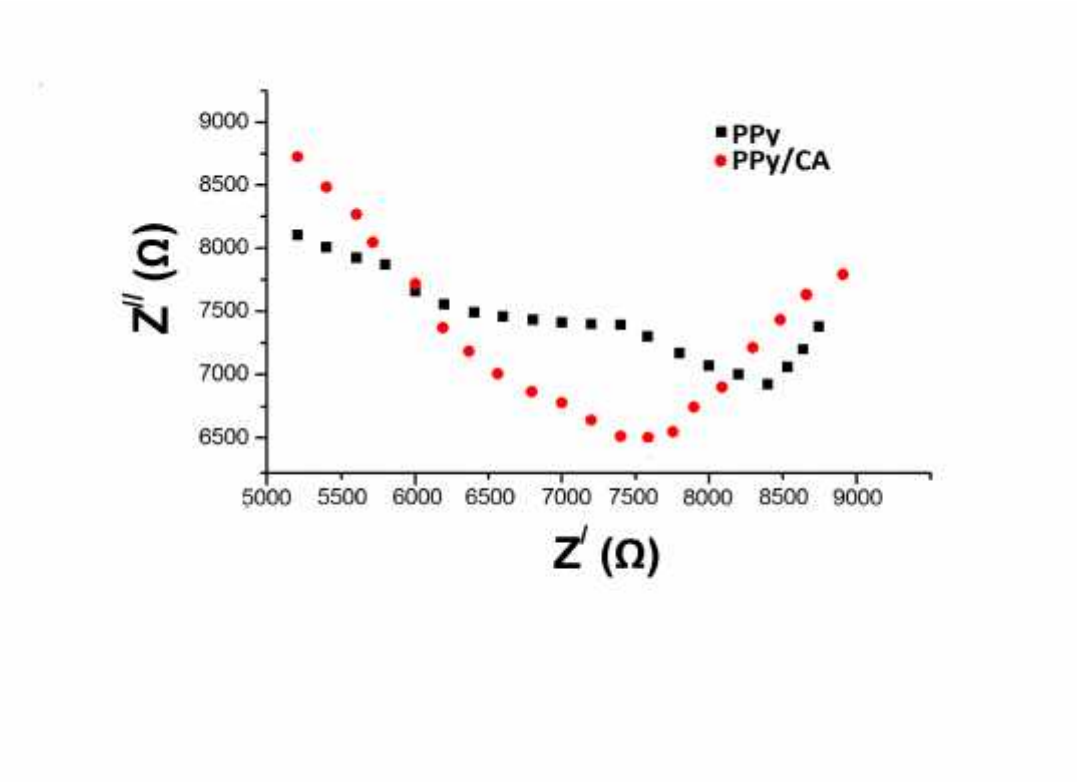

Fig 3.7 Nyquist plots for pure PPy and the PPy /CA composite

The ionic resistance of the material can be obtained by the following equation,

$$R_{ion} = 3\,(R_{low} - R_s) \quad \text{..... 3.1}$$

Where R_{low} is the real axis intercept of the vertical line at low frequency region of the spectra and R_s is the real axis intercept in that frequency range.

In contrast to pure PPy, the nano-composite shows no marked transition in the low frequency region. It was reported earlier that addition of the nano-particles leads to a catalytic effect and formed an electronic pathway for the polymerized composite [21]. Further, surface adsorption of nano particles inhibits one dimensional (1D) growth of PPy. This is evident from the morphology of the composite as shown in Figs.3.3 (b) and 3.4(b), showing that the morphology of the nano-composite is three dimensional (3D) and a compact one unlike PPy, which has shown 1D growth of its surface.

For this reason, the low frequency range of AC frequency (viz. 50Hz -500 Hz) has been chosen for sensing.

3.3.8 I-V measurement in the low frequency

The sensitivity of the polymer composite towards ethanol vapor is tested by recording room temperature change in I vs V with applied bias 0-4 Volt, and at different applied frequencies. I-V characteristics for four different frequencies with applied voltage 0-4V are shown in Fig.3.8, given below. We have taken the impedance spectra for low frequencies only, viz. 50 Hz, 100 Hz, 200 Hz and 500 Hz. Maximum current is observed in the lowest one (50 Hz) which gradually decreased with increasing frequency (i.e. 100 Hz, 200 Hz and 500 Hz). I-V shows a linear trend upto applied voltage of 1V in all the frequencies, while that trend gradually disappears in higher frequencies. However, in the composite a linear pattern is observed in the entire range of applied bias at 50 Hz, frequency with changeover to non linear nature in both the exposed and unexposed samples. The current response is minimum at 500 Hz. The result shows that impedance increases with frequency in the entire applied bias range.

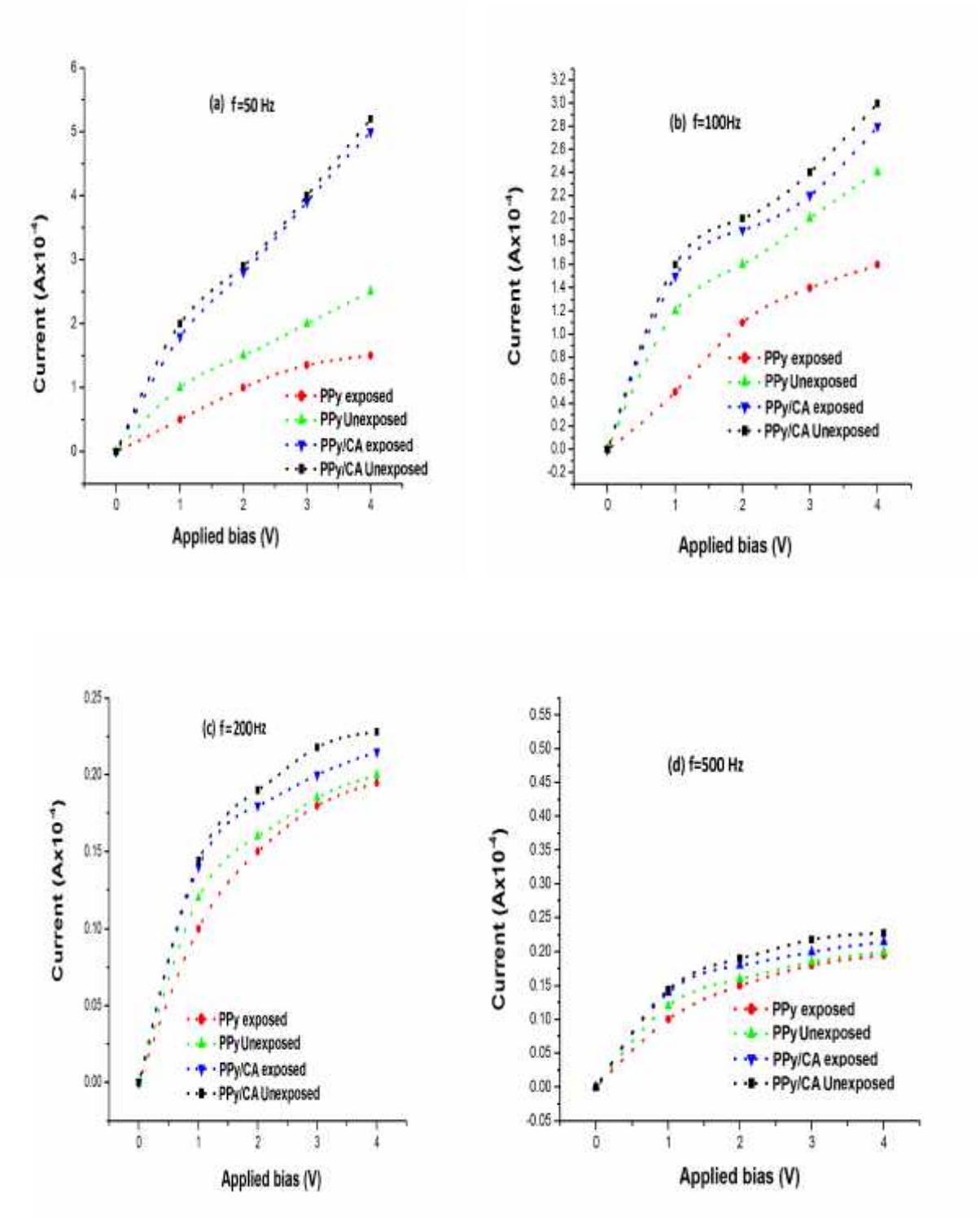

Fig.3.8 I-V characteristics of PPy and PPy/CA composite for applied frequencies of (a) 50Hz (b) 100 Hz (c) 200 Hz and (d) 500 Hz

3.3.9 Impedance measurements: ethanol sensitivity in terms of impedance

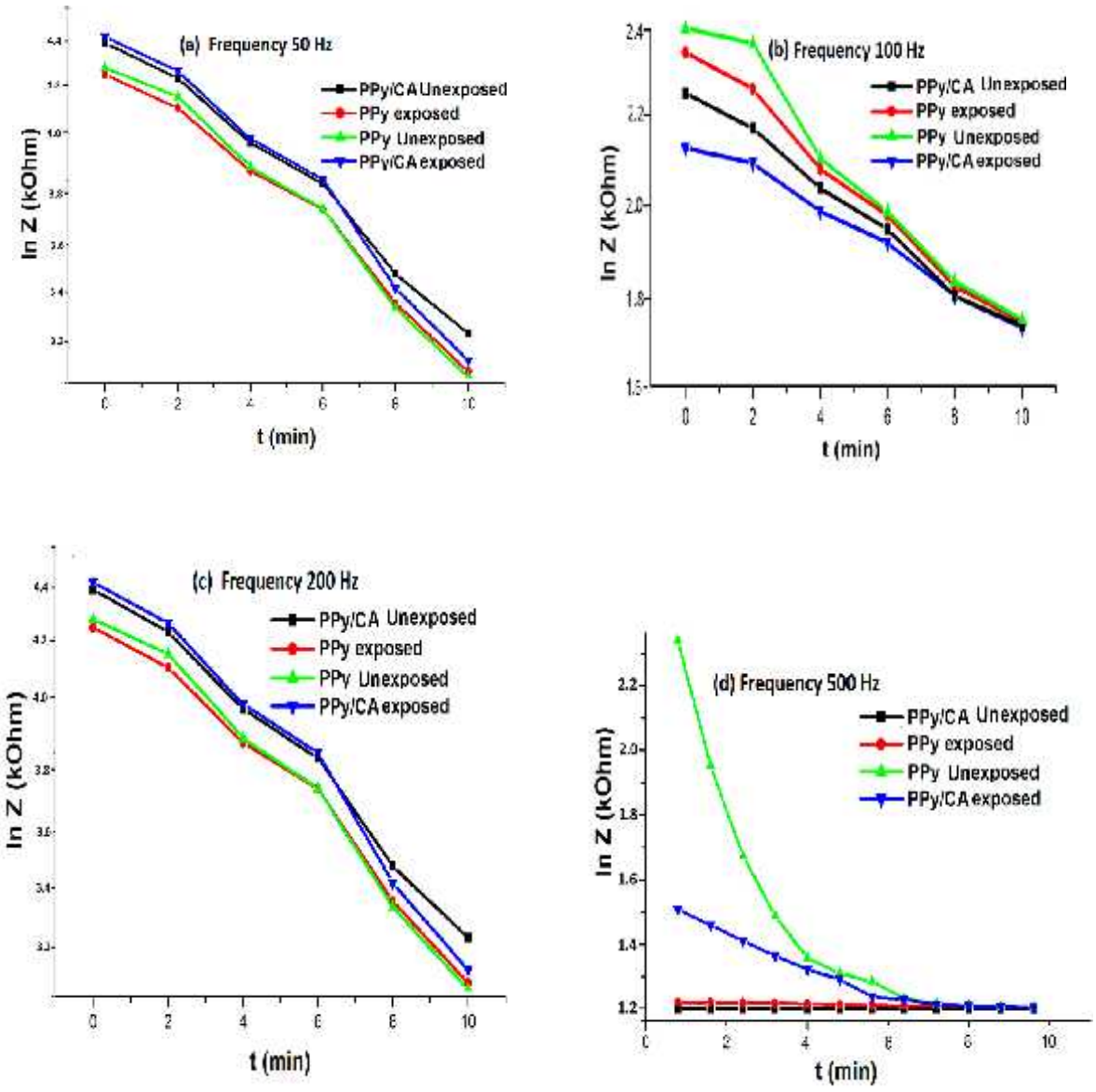

Fig. 3.9 **Impedance vs time in four different applied frequencies (a) 50Hz (b) 100 Hz (c) 200 Hz and (d) 500 Hz**

Along with the I-V characteristics, we have also observed how the impedance response (Z) of PPy and the composite changes with time at a particular bias voltage, in both the unexposed and the exposed states. The results are shown in Fig. 3.9 for Z vs time. The figure shows

decrease in Z with time as well as with frequency while a quite different nature is observed at applied frequency of 500 Hz.

3.3.10 Theory of Sensing:

(a) Physical: adsorption

In the interaction of bio-molecules with CP, intermolecular and surface forces act as mediator. These forces are broadly Van der Waals, electrostatic, hydrophobic and hydrogen bonding [22] and typically classified as Lifshitz Van der Waals (which is non polar, dispersive in nature) and Lewis acid base (which is polar in nature) force. Interaction of bio-molecule generally occurs immediately after its initial exposure in the material-liquid interface. Major limitation in the process is non-specific binding of the host molecule which determines selectivity needed in biosensor or actuator applications [23]. Specific interactions arise from a unique combination of forces that act in a directional manner forming, for instance, complimentary bonds [24] which may be stronger than the covalent bond existing between the CP and the dopant molecule. Though a lot of work has been done in the field of CP biosensor, very little information are found in literature which can serve as a quantifying model of the intermolecular and surface forces [25-27] and one has ample scope to analyze the adsorption and sensing behavior of the PPy composite dealt in the present dissertation.

According to Langmuir's adsorption theory, the gas molecules impinging on any solid surface do not generally rebounce but condense on the surface, being held by the interacting surface atoms and eventually evaporate from the surface. The time lag for evaporation depends on the intensity of the surface forces. Adsorption is the direct result of this time lag. The range of these surface forces is 10^{-10} m (i.e. the dimension of a molecule) [22]. Thus with the decreasing size of the molecules the dimension of the surface forces increases which can

hold the molecules in the surface. This happens in the present case when the PPy-CA composite is exposed to ethanol vapour. The oxygen from the OH group in ethanol has been getting attached with the hydrophilic sites generated by Cholic acid forming the "inner cavities" in the polymer composite which then undergo an ionic transformation leading to enhanced conductivity as shown in Fig.3.6 and 3.8. Selective adsorption of the bio-molecular composite is influenced by intermolecular and other competing forces which may result in decrease in interfacial interaction energy (E_{int}). Interfacial interaction plays a vital role in case of any bio-molecular incorporation in a CP and hence selective adsorption is observed when the CA incorporated PPy is exposed to ethanol vapor. It has been hypothesized that such interactions induces an alteration in the double helix of the polymer structure and subsequently allows formation of hydrogen bonds and intercalation of the polymer with formation of N-H bond as well as N-H- π interaction [28, 29] after exposure to ethanol vapor, resulting in subsequent changes in conductivity as shown by the I-V characteristics.

(b) Chemical

At first Oxygen is adsorbed on the composite surface. The adsorbed oxygen forms ionic species O^- , O^{2-} and O_2^- which acquire electrons from the PPy surface; PPy being a good electron donor with delocalized electron [30]. The polymer blend undergoes a chemical change on exposure to ethanol vapor. The interaction taking place in between the aromatic rings of the polymer and the ionic species of Oxygen (O^- , O^{2-} and O_2^-) is non covalent in nature and was studied by Germain et al and introduced the term 'π-stacking' [31] to describe it. Electrons participating in such interactions are free to migrate into the polymer surface and results in its increased conductivity.

The reaction kinematics may be expressed as [32],

$$O_2\,(gas) <=> O_2\,(adsorbed)$$

$$O_2\,(adsorbed) + e^- <=> O_2^-$$

$$O_2^- + e^- <=> 2O^-$$

The reaction between ethanol and ionic oxygen can take place in two different ways:

$$C_2\,H_5OH\,(gas) + O^- <=> CH_3CHO + H_2O + e^-$$

$$C_2H_5OH\,(gas) <=> H+C_2H_5O\,(surface)$$

$$C_2H_5O <=> H+ CH_3CHO$$

$$CH_3CHO + O\,(bulk) \rightarrow CH_3COOH + O\,(vacancies)$$

The conductivity arises from electron transfer along the conjugated π-molecular backbone coupled with the motion of the charge carriers after exposure to ethanol vapour. On oxidation, an electron is removed from the π- system producing a cation which constitutes a polaron when associated with the local distortion. Thus a polaron is formed in every four pyrrole unit. On further oxidation, pairs of polarons combine to form bipolarons which are

energetically more favourable. Bipolarons can migrate along the polymer chain providing the charge transport in the PPy structure [33]. The conductivity is however determined by the charge transfer between the dopant and the remaining part of the polymer segment: charge carrier mobility within a single polymer chain and charge transfer (i.e. hopping) between different polymer chains [34]. The exposure to ethanol enhances the charge carrier mobility in the CP which is further stimulated by incorporation of CA in the polymer [35].

3.4 Conclusion

Incorporation of Cholic Acid on DBSA doped PPy results in the formation of a polymer composite with a supra-molecular structure with imprinted properties of PPy as well as Cholic Acid. Certain properties are modified to incorporate in topography and electronic conductivity of the composite, probably due to formation of certain complimentary bonds stronger than the covalent bonds caused by interaction of the surface forces when Cholic Acid is incorporated in the polymer. On incorporation of Cholic acid multi layered surface topography is observed with the formation of nano sheet. Change in conductivity is also observed due to enhanced surface charges in the form of polarons and bipolarons with incorporation of the bio-molecule. The change is prominent when the composite is exposed to ethanol vapor, due to protonation of the oxygen molecules in the OH group of ethanol, adsorbed in the surface cavities of the composite. Both resistance and impedance of the of the polymer composite show characteristic changes on ethanol exposure which is stronger in the lower frequency range. The change in impedance is most prominent in 50 Hz when the current is found maximum and linearity is observed in the low frequency range in the applied bias range of 0 to 1Volt. With increasing frequency the I-V curves show gradual decrease in the value of current for the same applied bias indicating increasing value of impedance, which is normal in case of CP's like PPy. AC conductivity of CP's increases with increasing

electronic mobility till a saturation level is reached and inter chain hopping continues which is stimulated by the frequency of the applied field. Cholic Acid incorporation possibly causes surface modification of the polymer which facilitates electronic mobility and on exposure to an ionizing vapor (e.g. ethyl alcohol), the saturation level is reached at a very low frequency.

3.5 Reference

1. M. Axelson, E. Ellis, B. Mörk, K. Garmark , A. Abrahamsson, I. Björkhem, B. G. Ericzon and C. Einarsson. *Hepatology*. 31, 2000, 1305.

2. A K Bandyopadhyaya, N. M. Sangeetha and U. J. Maitra. *Org Chem*. 65, 2000, 8239.

3. V. H. Soto Tellini, A. Jover, L. Galantini, N.V. Pavel, F. Meijide and J. Vázquez Tato. *J Phys Chem B.* 110, 2006, 13679.

4. V.H.Soto Tellini, A. Jover, F. Meijide, J. Vázquez Tato, L. Galantini and N.V. Pavel. *Adv Mater*. 19, 2007, 1752.

5. P. Babu, N. M. Sangeetha and U. Maitra. *Macromol Symp*. 241, 2006, 60.

6. A. P. Davis and J. B. Joos. *Coord Chem Rev*. 240, 2003, 143.

7. S. Ghosh, A. R. Choudhury, T. N. Guru Row and U. Maitra. *Org Lett*. 7, 2005, 1441.

8. M. Yoshii, M. Yamamura, A. Satake and Y. Kobuke. *Org Biomol Chem*. 2, 2004, 2619.

9. M. Alvarez Alcalde, A. Jover, F. Meijide, L. Galantini, N.V. Pavel, A. Antelo and J. Vázquez Tato. *Langmuir*. 24, 2008, 6060.

10.X. X. Zhu and M. Nichifor. *Acc Chem Res*, 35, 2002, 539.

11.X. Z. Hu, Z. Zhang, X. Zhang, Z Y Li, Z. X. Xhu. *Steroids*, 2005, 70: 531.

12.M. Ahlheim, M. L. Hallensleben. *Makromol Chem, Rapid Commun*, 1988, 9: 299.

13. P.P D. Sharma and D. Sarkar. *Ind J Biochem Biophys* 52 (2), 2015, 203.

14.R.M.Silverstein, G.C. Bassler, T. C. Morrill. Spectroscopic identification of organic compounds. 5th edn, Wiley, 1992

15. The Aldrich Library of FTIR spectra, 1997

16. A. Benrebouh, D Avoce and X. X Zhu. *Polymer* 42, 2001, 4031.

17 A. Gelmi, M.J. Higgins and G. G. Wallace. *Biochim. Biophys. Acta* doi:pii: S0304-4165(13), 2013, 00083-4.

18. A. Gelmi, M. Zanoni, M. J Higgins, S, Gambir, D. L Officer, D. Diamond and G. G. Wallace,

J. Mater. Chem. B. 1, 2013, 2162.

19. G. Garcia-Belmonte, J. Bisquert, *Electrochim. Acta*, 47, 2002, 4263

20. X. Ren and G. Pickup. *J. Phys. Chem*., 97, 1993, 5356

21. Y.C. Liu and C.J. Tsai, *J. Electroanal. Chem*., 537, 2002,165

22. D. Leckband and J.Israelachvili, *Quart. Rev. Biophys*. 34, 2001, 105.

23. M. Gerard, A. Chaubey and B.D. Malhotra, *Biosens. Bioelectron*. 17, 2002, 345.

24. X .Yang, C.O. Too, L. Sparrow, J. Ramshaw and G.G. Wallace, *React. Func. Polym.* 53, 2002, 53.

25. X. Cui, V.A.Lee, Y. Raphael. J.A Wiler, J. F. Hetke, D. J Anderson and D. C Martin *J. Biomed. Mater*. Res. 56, 2001, 261.

26. C. Saltó, E Saindon, M. Bolin, A. Kanciurzewska, M. Fahlman,E. W Jager and P Tengvall. *Langmuir*, 24, 2008, 14133.

27. S Cosnier and M. Holzinger, *Chem. Soc. Rev*. 2011, 40, 2146.

28. J Preat, B. Teixeira-Dias, C. Michaux, E. A Perpète and C. Alemán, *J. Phys. Chem. A*, 2011, 115, 13642.

29. J. Preat, D. Zanuy, E. A Perpète and C. Alemán, *Biomacromolecules*, 201,12, 1298.

30. L. Misevicˇiene˙, Zˇ. Anuseviˇcius and J. N. Sarlauskas, *Acta Biochimica Polinica* 53, 2006, 569.

31. M.E. Germain and M.J. Knapp, *Journal of the American Chemical Society* 130, 2008, 5422.

32. H F Hellegourac, F Aefi Khonsari, P R lanadeand and J. Amourax. *Sens Actuat B*, 73, 2001, 27.

33. G. Inzelt, M.Pineri, J. W. Schultze, and M. A. Vorotyntsev, Electrochim. Acta 45, 2000, 2403.

34. A. Bhattacharya, A. De and S. Das, *Polymer* 34, 1996, 4375.

35. A. N Papathanassiou, J. Grammatikakis, I. Sakellis, S. Sakkopoulos, E.Vitoratos and E. Dalas, *Appl. Phys. Lett*. 87, 2005, 154